JOURNAL OF Materials CHEMISTRY

Inter-ring interactions and peripheral tail effects on the discotic mesomorphism of 'free-base' and Co(II), Ni(II) and Cu(II) alkenyl(sulfanyl) porphyrazines

Sandra Belviso, Giampaolo Ricciardi* and Francesco Lelj*

Dipartimento di Chimica and Laboratorio per i Materiali Innovativi (LaMI), Università della Basilicata, Via N. Sauro 85, 85100 Potenza, Italy

Received 15th September 1999, Accepted 26th October 1999

The self-organizing capability of a family of newly synthesized 'free-base', H_2(OASPz), and metal porphyrazines, M(OASPz) ($OASPz^{2-}$ = 2,3,7,8,12,13,17,18-octakis(alkenylthio)-5,10,15,20-tetraazaporphyrinato dianion, n = 4, 5, 6, 8; M = Co, Ni, Cu), into columnar, discotic liquid crystals, has been investigated by differential scanning calorimetry (DSC), optical microscopy and X-ray diffraction. It is found that of the metal-free porphyrazines only those with n = 4 or 5 show, as indicated by X-ray and optical microscopy studies, characteristic stable and discotic nematic mesophases. All the metallated porphyrazines show a discotic liquid crystalline behavior and those with the largest values of n present, consistent with the X-ray results, hexagonal columnar packing. Comparing the mesomorphic behavior of these compounds with those of the parent compounds peripherally substituted with saturated alkyl(sulfanyl)-chains it is seen that the effect of the increased stiffness at the periphery of the chains, induced in the title tetrapyrroles by the terminal double bonds, results in a decrease of the clearing temperature, T_i, and also of the mesophase temperature stability range, ΔT. This effect is larger in H_2 and Ni than in Cu and especially in Co porphyrazines, where the axial coordinating capability of the Co seems to counterbalance the effect of this perturbation.

Introduction

The hybrid structure of the porphyrazinato ligand, which can be regarded as derived from the porphyrin ring where the methine bridges are replaced by aza bridges, causes the physical and chemical properties of 'free-base' and transition metal porphyrazines to be peculiar in many cases. A number of recent investigations have indicated that porphyrazines show a rich coordination chemistry, excellent chemical, thermal and photochemical stability and a variety of technological applications of these macrocycles have been actively investigated depending on the nature of the peripheral substituents and the central metal ion, such as liquid crystals (LC), Langmuir–Blodgett (LB) films, electrocatalysis and photodynamic cancer therapy, among others.[1–7]

Of the different types of porphyrazine-like macrocycles, the alkyl(sulfanyl)porphyrazines, a family of compounds where thioether-groups are attached at the β-positions of the azaporphyrin ring, present attractive characteristics in terms of their electrochemical and optical properties and versatility and architectural flexibility that allow the tailoring of the physico-chemical parameters.[2,8–10]

Alkyl(thio)porphyrazines present high self-organizing capabilities to form different types of condensed phases such as discotic LC and LB films, mainly owing to appreciable π–π interactions between the aromatic rings (for the 'free-base' azaporphyrins) or to concurrent π–π interactions between the aromatic rings and metal–sulfur interactions between adjacent rings (for metalloporphyrazines) (Fig. 1).[2g–m,11–14]

The remarkable molecular flexibility of the octakis(alkyl)sulfanylporphyrazine ring (Fig. 1), and the knowledge that the structural and optical properties of the azaporphyrin ring can be finely adjusted by synthetic means, make (alkyl)sulfanylporphyrazine derivatives especially suitable to investigate in detail the molecular self-organizing phenomena of tetrapyrroles in order to find connections between the molecular structure and the occurrence of mesophases with possible applications in opto-electronic technology.[2d,11,15–18]

In a recent paper, we have studied the mesomorphic behavior of transition metal complexes of octakis alkyl(sulfanyl)porphyrazines.[2m] The results of this investigation have provided a detailed pattern of the individual role of the size of the peripheral tails and of the nature of the metal on the structure and stability of the LC state. It was observed in particular that, for a given transition metal the larger the size of the peripheral organic chains the lower is the thermal stability range of the mesophase. Furthermore, it was found that, unlike in phthalocyanine- and porphyrin-based discotic LCs, where the stability of the mesophases is not immediately related to the

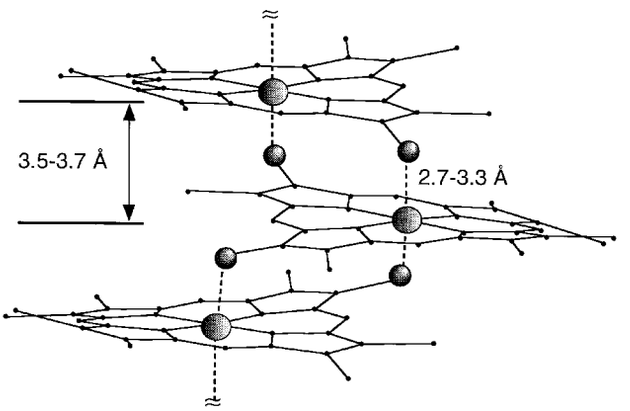

Fig. 1 Edge-on view of the M(OASPz) M···S extraplanar interactions in the crystal (M = Fe, Mn, Co) identified by single-crystal X-ray structure determination.[8–10] The ball and stick drawing illustrates also the saddle-like ruffling of the M–porphyrazine–octathiolato moiety of the M(OASPz) molecules viewed down a M–N_p bond. Peripheral alkyl chains are omitted for clarity. Metal and sulfur atoms engaged in the axial M···S interactions are represented by enlarged balls.

nature of the coordinated metal, the thermal stability of the mesophase increases with the capability of the coordinated metal to show axial unsaturation.[2m,19–21]

The present paper deals with the synthesis, characterization and discotic mesomorphism of 'free base' and Co(II), Ni(II) and Cu(II) complexes of 2,3,7,8,12,13,17,18-octakis(alkenylsulfanyl)-5,10,15,20-porphyrazines ($n=4,5,6,8$), a class of compounds which differs from that previously studied owing to the presence of a terminal double bond in each of the peripheral organic tails. The chemical structure of a typical porphyrazine with $n=4$ is shown in Chart 1. Our first aim is to provide a quantitative estimate of the effects of unsaturation in the peripheral chains and of the inter-ring interactions, on the mesomorphic behavior of these compounds. For this purpose, a comparison of the mesomorphic behavior of the title porphyrazines with those previously studied will be of some help.

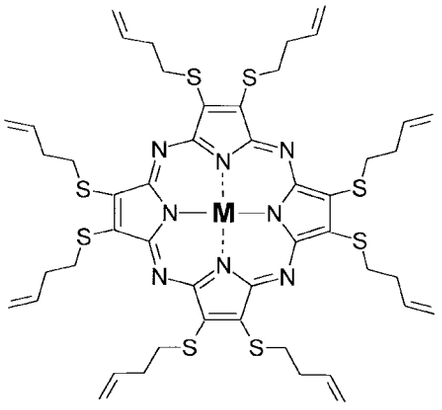

M(OASPz) **M = Co, Ni, Cu**

Chart 1

Getting insight in this topic is important for at least two reasons: first, if the unsaturation preserves the relevant mesomorphic features of these tetrapyrrole complexes, they can be used as precursors for polymeric discotic LCs.[22–24] By combining the polymerization capability of the peripheral double bond (inter-columnar linkages involving a reaction between the terminal double bonds can be easily promoted photochemically and/or by a radical initiator) with possible inter-ring M···S axial interactions, 2D and even 3D architectures of the mesophases could be obtained.

Second, since the present work represents the first systematic investigation on the effects that the increased stiffness of the peripheral chains induced by terminal double bonds may have on the discotic mesomorphism of porphyrazine based LCs, our results may provide useful experimental trends and suggestions to model theoretically these and similar systems.[25]

Experimental

Instrumentation

All chemicals and solvents (Aldrich Chemicals Ltd.) were of reagent grade and used in the syntheses as supplied. Solvents used in physical measurements were of spectroscopic or HPLC grade.

Microanalyses were performed by Butterworth Laboratories Ltd, Teddington, UK. Solution electronic spectra in 1 or 10 cm path length quartz cells in the region 200–2500 nm were performed on a UV–Vis–NIR 05E Cary spectrophotometer. The proton ^{1}H NMR spectra were recorded on an AM 300 MHz Bruker spectrometer with $SiMe_4$ as internal standard.

Optical observations of textures as a function of the temperature were performed with a Axioplan-Zeiss polarizing microscope equipped with a Linkam microfurnace. Samples were studied between silica glass plates (diameter 16.0 mm).

Transition temperatures were measured by differential scanning calorimetry with a Perkin Elmer DSC7 (series 1020) instrument operated at scanning rates of 5 and 10 °C min^{-1}. The apparatus was calibrated with indium (429.6 K, 28.4 J g^{-1}) as standard. The sample pans and covers were made of aluminium (diameter 5.0 mm). The uncertainty in each measured temperature was ± 0.1 °C. X-Ray diffraction experiments were carried out using a monochromatic Cu-Kα beam. The diffraction patterns were recorded by a photographic method (Rigaku flat film camera) utilizing a temperature controlled microfurnace. Samples were kept under a dry nitrogen atmosphere in sealed Lindemann glass capillaries (diameter 1.0 mm) at the appropriate temperature that was constant within ± 1 °C.

Syntheses

All the metal free porphyrazines were prepared by a modification of the method used by Schramm and Hoffmann for the synthesis of 2,3,7,8,12,13,17,18-octakis(methylthio)porphyrazine.[2d] Since the synthetic procedure did not change significantly going from one porphyrazine to another, in the following we report the synthetic details only for the porphyrazine with $n=4$ taken as an example. Furthermore, since the synthetic procedure for metal porphyrazines did not change for a given metal with the size of the peripheral tails on the porphyrazinato ligand, we describe here, for each metal, only the details concerning the synthesis of the complex with $n=4$ as a typical synthetic experiment.

2,3,7,8,12,13,17,18-Octakis(but-3-enylthio)-5,10,15,20–21*H*, 23*H*-porphyrazine, H_2(OASPz). Disodium *cis*-1,2-dicyano-1,2-ethylenedithiolate **1** was prepared according to the procedure reported in the literature.[2e] 1,2-Dicyano-1,2-bis(but-3-enylthio)-ethylene **2** was obtained by the procedure of Bahr and Schleiter[2e] with some modifications. 5.0 g (37.0 mmol) of CH_2=$CHCH_2$-CH_2Br, dissolved in methanol (5.0 mL), were added dropwise to a vigorously stirred suspension of **1** (3.4 g, 18.5 mmol) in methanol (10.0 mL) cooled by a water–ice bath (0 °C). The temperature was increased to 25 °C and the solution was stirred continuously for 24 h. After removal of the solvent under vacuum, the compound was dissolved in $CHCl_3$, washed by water, dried over Na_2SO_4 and filtered. The compound, freed of the solvent using a rotary evaporator, appeared as a very malleable brown solid. The absence of alkenyl halide was checked by NMR. The yield of the reaction was $>70\%$.

[2,3,7,8,12,13,17,18-Octakis(but-3-enylthio)-5,10,15,20-porphyrazinato]magnesium(II), Mg(OASPz) 3. 0.30 g of Mg powder, previously washed with diethyl ether and dried, were refluxed ($T=120$ °C) overnight in *n*-propanol (50.0 mL). Compound **2** was added to the suspension under stirring and the solution was refluxed for 36 h. Subsequent addition of water to the cooled reaction mixture led to a dark green solid that was collected by filtration and passed through a column of silica gel (Merck 60, 70–230 mesh) using CH_2Cl_2–*n*-hexane (1 : 1) as eluent (first band) (Yield 70%).

Pure solid **3** was dissolved in $CHCl_3$, filtered and transferred in a separating funnel. Successively, CF_3CO_2H–$CHCl_3$ (1 : 2) was added in portions of 3.0 mL until the solution turned from green to blue. The solution was then washed with a NaOH solution (0.5 M) and with water until the washing water was fully neutralized. The dark product was dried over sodium sulfate and filtered. After removal of the solvent, the crude product was carefully purified by flash chromatography on silica gel (Merck 60, 70–230 mesh) using CH_2Cl_2–*n*-hexane

(1 : 1) as eluent (first band). The free-base porphyrazine was obtained in a yield of *ca.* 70% with respect to Mg(OASPz).

[2,3,7,8,12,13,17,18-Octakis(but-3-enylthio)-5,10,15,20-porphyrazinato]copper(II), Cu(OASPz). 0.10 g (0.10 mmol) of H_2(OASPz) were dissolved in $ClCH_2CH_2OH$ (10.0 mL). A warm solution of 0.02 g (0.10 mmol, an excess of 20% respect to a 1 : 1 molar ratio) of $(CH_3CO_2)_2Cu\cdot H_2O$ in EtOH (3.0 mL) was added and the mixture was refluxed at 110 °C for 1 h under magnetic stirring. The progressive formation of the metal complex was monitored through UV–VIS spectroscopy. After cooling, a precipitate was obtained by addition of MeOH (5.0 mL) to the reaction mixture and freezing at 0 °C for 12 h. The precipitate was collected under vacuum filtration, washed with MeOH and then purified by column chromatography on silica gel (Merck 60, 70–230 mesh) using CH_2Cl_2–*n*-hexane (1 : 1) as eluent (first band). Removal of the solvent and recrystallization from CH_3OH–CH_2Cl_2 (9 : 1) at *ca.* 0 °C gave 0.060 g (*ca.* 57%) of the pure blue product.

[2,3,7,8,12,13,17,18-Octakis(but-3-enylthio)-5,10,15,20-porphyrazinato]nickel(II), Ni(OASPz). 0.10 g (0.10 mmol) of the free-base porphyrazine with $n=4$ were dissolved in 1,4-dioxane–EtOH (1 : 1) (12.0 mL) under magnetic stirring at 110 °C. 0.018 g (0.13 mmol, an excess of 30% with respect to a 1 : 1 molar ratio) of $CH_3CO_2Na\cdot 3H_2O$ and then a warm solution of 0.060 g of $NiCl_2\cdot$dme (dme = dimethoxyethane) in 1,4-dioxane–EtOH (1 : 1) (5.0 mL) were added. The reaction mixture was refluxed at 100 °C for 20 min and the progressive formation of the metal complex was monitored *via* UV–VIS spectroscopy. The solvent was removed from the residual slurry under high vacuum, leading to a dark solid that was passed through a column of silica gel (Merck 60, 70–230 mesh) using CH_2Cl_2–*n*-hexane (1 : 1) as eluent (first band). Removal of the solvent and recrystallization from CH_3OH–CH_2Cl_2 (9 : 1) at *ca.* 0 °C gave 0.050 g (*ca.* 47%) of the desired pure dark blue product.

[2,3,7,8,12,13,17,18-Octakis(but-3-enylthio)-5,10,15,20-porphyrazinato]cobalt(II), Co(OASPz). 0.10 g (0.10 mmol) of H_2(OASPz) with $n=4$ were dissolved in a stirred 1,4-dioxane–EtOH (1 : 4) solution (12.0 mL) at 110 °C. 0.014 g (0.10 mmol) of $CH_3CO_2Na\cdot 3H_2O$ and then a warm solution of 0.03 g (0.14 mmol) of $CoBr_2\cdot H_2O$ (a large excess with respect to a 1 : 1 molar ratio) in 1,4-dioxane–EtOH (1 : 4) (3.0 mL) were added. The reaction mixture was refluxed at 100 °C for 2 h and the progressive formation of the metal complex was monitored *via* UV–VIS spectroscopy. The reaction mixture was freed of the solvent under rotary evaporation and the crude product was purified by column chromatography on silica gel (Merck 60, 70–230 mesh) using a gradient technique. Using an initial CH_2Cl_2–*n*-hexane (2 : 3) mixture as eluent, a blue band was collected corresponding to the unreacted free-base porphyrazine. The slow moving band corresponding to the desired compound was collected using CH_2Cl_2–*n*-hexane (1 : 1) as eluent. Removal of the solvent and recrystallization of the residue by slow evaporation of the solvent from a *n*-pentane–CH_2Cl_2 (9 : 1) solution of the cobalt complex gave 0.025 g (*ca.* 23%) of the pure green product.

Results and discussion

Synthesis and general characterization

The synthetic procedure used to prepare azaporphyrin macrocycles with peripheral tails containing terminal unsaturation is very similar to that used for the preparation of the saturated analogs and needs only a few additional modifications.[2h]

The 'free-base' derivatives are obtained in a rather low yield, though comparable to the yields achieved for the synthesis of the azaporphyrins containing saturated tails.

A clean demetallation reaction of the Mg(OASPz) precursor derivatives was obtained using trifluoroacetic acid–chloroform (1 : 2) as a magnesium 'stripping' agent, in the place of pure trifluoroacetic acid.[2m] The use of pure trifluoroacetic acid led to the formation of a number of by-products, which were difficult to remove by conventional chromatographic techniques.

As for the metal complexation reactions, we noted that the insertion of Cu ion in the azaporphyrin cavity was very fast in 2-chloroethanol, a very useful solvent in the synthesis of alkylthioporphyrazines, whatever is the length of the peripheral chains, whereas the insertion of Co and Ni metal ions is a slow and low yield reaction (yields of *ca.* 10% are obtained after 1 d). We have found that the yields can be improved (up to 30%) by refluxing the nickel chloride dimethoxyethane adduct and $CoBr_2$, respectively, in a 1,4-dioxane–ethanol mixture as solvent.

As indicated in Table 1, metal-free and metallated porphyrazines gave satisfactory analytical data. Diamagnetic compounds, *i.e.* 'free-base' and nickel porphyrazines, were characterized by ^{1}H NMR spectra the results of which are collected in Table 2. The spectra showed, besides typical resonances of the terminal double bond in the range δ 4.8–6.0 characteristic signals due to the remaining methylene groups in

Table 1 Elemental analysis data (%) for the H_2(OASPz) and M(OASPz) compounds

		C		H		N	
	n	Found	Calc.	Found	Calc.	Found	Calc.
H_2	4	56.90	57.45	5.94	5.83	10.94	11.16
	5	60.87	60.28	6.84	6.68	9.74	10.04
	6	63.10	62.60	7.66	7.39	8.82	9.12
	8	65.65	66.16	8.33	8.47	6.97	7.71
Co	4	54.22	54.37	5.09	5.32	10.22	10.57
	5	57.21	57.36	5.97	6.19	9.22	9.56
	6	59.27	59.83	6.53	6.90	8.18	8.72
	8	63.51	63.66	7.78	8.01	7.07	7.42
Cu	4	53.49	54.13	5.07	5.30	9.86	10.52
	5	57.11	57.13	5.59	6.16	9.07	9.52
	6	59.31	59.61	6.42	6.88	8.10	8.69
	8	62.89	63.47	7.45	7.99	7.00	7.40
Ni	4	53.86	54.38	5.50	5.32	9.94	10.57
	5	56.76	57.37	5.88	6.19	8.95	9.56
	6	59.45	59.84	6.60	6.90	8.27	8.72
	8	63.05	63.67	7.65	8.01	6.88	7.42

Table 2 ^{1}H NMR spectroscopic data (δ_H; $CDCl_3$) for the diamagnetic compounds[a]

	n	SCH_2	$-CH_2-$	$-CH_2-$	$-CH_2-$	$-CH_2-$	$-CH_2-$	HC=	CH_2=
H_2	4	4.71 t	2.66 m	—	—	—	—	6.01 m	5.11 dq
	5	4.11 t	2.37 m	1.98 m	—	—	—	5.81 m	4.99 dq
	6	4.11 t	2.09 m	1.91 m	1.72 m	—	—	5.76 m	4.91 m
	8	4.10 t	2.00 m	1.88 m	1.61 m	1.35 m	1.35 m	5.72 m	4.88 m
Ni	4	4.08 t	2.61 m	—	—	—	—	5.99 m	5.11 dq
	5	4.02 t	2.34 m	1.94 m	—	—	—	5.78 m	4.99 dq
	6	4.02 t	2.06 m	1.86 m	1.61	1.61	—	5.74 m	4.90 dq
	8	4.01 t	1.98 m	1.84 m	1.58 t	1.58 t	1.31 m	5.70 m	4.87 dq

[a]t = triplet; dq = double quartet; m = multiplet.

the range δ 1.3–2.7. The presence of alkylene isomers was excluded on the basis of ^{1}H NMR spectra.

The optical spectra of 'free-base' and metallated alkenyl-(sulfanyl)porphyrazines, the relevant features of which are reported in Table 3, are dominated by two intense bands, the Q-band (located in the range 640–717 nm) and the B-band in the near UV region (located in the range 330–370 nm) both correlated to π–π transitions (see also Fig. 2 where the UV–VIS spectra of H_2(OASPz) and M(OASPz) compounds with $n=6$ are shown). Charge transfer (CT) and $n_{sulfur} \rightarrow \pi^*$ transitions of variable intensity and energy lie in between. It is notable that all the spectral features show significant breadth owing to intermolecular interactions, which are present even at very low concentrations (the aggregation limit is below 10^{-6} M). The Soret band is, in particular, clearly split into two components owing to intermolecular exciton-like interactions.[2]

Phase behavior

Phase transition temperatures and enthalpy data for the 'free bases' and the corresponding metal complexes are gathered in Tables 4 and 5, respectively. Of the 'free-base' porphyrazines, only those with $n=4$ or 5 showed liquid crystalline behavior, whereas all the metal complexes investigated here formed liquid crystals. We notice that, as inferred from a polarized light analysis, the cobalt complexes with $n=4$ and 5 and the copper complex with $n=4$ decompose at the clearing point or immediately past the transition to isotropic liquid. For this reason, for these complexes, the mesophase→liquid transition

Table 3 UV–VIS spectroscopic data in $CHCl_3$ for the H_2(OASPz) and M(OASPz) compounds. λ_{max}/nm (log ε/dm^3 mol^{-1} cm^{-1})[a]

		n			
		4	5	6	8
H_2	Q	715 (4.82) 648 (4.63) 635 (sh) (4.62)	713 (4.41) 643 (4.24)	713 (4.01) 643 (3.86) 616 (sh) (3.77)	714 (4.46) 654 (sh) (4.27) 647 (4.30) 634 (sh) (4.27)
	Extra	510 (4.43)	512 (4.10)	530 (sh) (3.72) 508 (3.74)	514 (4.06)
	Soret	360 (4.85) 340 (sh) (4.85)	362 (4.41) 352 (4.41)	365 (4.00) 338 (4.00)	364 (sh) (4.41) 349 (sh) (4.41) 344 (4.43)
Co	Q	645 (4.71)	646 (4.59) 600 (sh) (4.34)	652 (3.97) 624 (sh) (3.88) 597 (sh) (3.68)	664 (sh) (4.36) 649 (4.38)
	Extra	483 (4.16) 440 (4.16)	491 (4.10) 450 (4.02)	484 (3.30) 448 (3.30)	489 sh (3.70)
	Soret	330 (4.69)	331 (4.54)	347 (sh) (3.91) 330 (3.94)	389 (sh) (4.02) 344 (4.31)
Ni	Q	720 (sh) (4.26) 665 (4.58) 650 (sh) (4.55) 630 (sh) (4.40) 570 (sh) (4.06)	670 (4.03) 619 (sh) (3.90)	667 (3.96) 622 (sh) (3.81)	680 (sh) (4.39) 666 (4.41) 641 (sh) (4.33) 619 (sh) (4.26)
	Extra	485 (4.13)	489 (3.73)	490 (3.59)	509 (sh) (3.97) 490 (4.06)
	Soret	325 (4.58)	341 (sh) (4.00) 325 (4.03)	345 (sh) (3.94) 324 (3.99)	347 (sh) (4.37) 320 (4.42)
Cu	Q	675 (4.87) 636 (sh) (4.54)	672 (4.65) 629 (sh) (4.30)	678 (3.82) 630 (sh) (3.66)	674 (4.65) 619 (sh) (4.23)
	Extra	500 (4.29)	499 (4.13)	504 (3.54)	504 (4.01) 489 (sh) (3.99)
	Soret	355 (4.70) 340 (4.72)	356 (4.50)	358 (sh) (3.77) 337 (3.78)	359 (sh) (4.39) 344 (4.48)

[a]sh = shoulder.

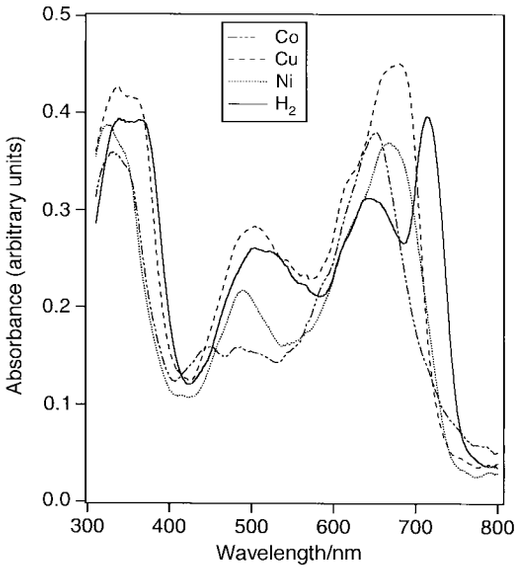

Fig. 2 UV–VIS spectra of H_2(OASPz) and M(OASPz) compounds with $n=6$, in $CHCl_3$. For H_2(OASPz), $c=2.93\times10^{-5}$ M; Co(OASPz), $c=2.99\times10^{-5}$ M; Ni(OASPz), $c=2.98\times10^{-5}$ M; Cu(OASPz), $c=5.33\times10^{-5}$ M.

was not detected by DSC and the relative enthalpy data are not available.

The calorimetric analysis indicates that, in general, the mesomorphism is enantiotropic. In fact, with the exclusion of the series with $n=4$ which is probably affected by kinetic difficulties in the crystallization, the reverse phase transformations are usually well resolved although some supercooling of the isotropic liquid does regularly occur.

Most of the compounds, especially those of the series with $n=5$, exhibit solid polymorphism. Normally we observed, for a given sample, the concomitant presence of two solid phases, one of which is metastable, formed either by solution crystallization or by melt crystallization. Since the central point of this paper, however, concerns the liquid-crystalline behavior of the porhyrazines, we shall not discuss the solid polymorphism in much detail, except for a few rather peculiar cases.

The DSC heating curve of H_2(OASPz) with $n=5$ crystallized from solution is shown in Fig. 3(a). The peak temperature corresponding to the melting endotherm lies at 73.9 °C and the associated enthalpy change amounts to 21.8 J g^{-1} and is preceded by a thermally detectable transformation of an unknown nature at 70.7 °C with an enthalpy change of 2.1 J g^{-1}. In the subsequent cooling experiment, the crystallization of the mesophase [Fig. 3(b)] is characterized by a single exothermic peak. The successive heating DSC run [Fig. 3(c)] obtained after a thermal treatment of the melt crystallized sample at 60 °C for 30 min, shows how the annealing process has promoted the reorganization of the solid phase. The enthalpy change, in fact associated to the first phase transition (now at 70.8 °C) increases to 20.2 J g^{-1} whereas that of the second, at 73.6 °C, decreases to 17.4 J g^{-1}.

Both temperatures and enthalpy changes of the phase transitions vary regularly with the size [identified by the number (n) of carbon atoms] of the alkenyl chains and the coordinated metal. For a better evaluation of the effect of these parameters and, in particular, of the terminal double bond in the tails, on the stability and structure of the mesophases, we compare the data with those obtained for the corresponding porphyrazines with saturated peripheral chains, when available. To this end the peak temperatures of the solid→mesophase (T_m) and mesophase→liquid (T_i) transitions together with the thermal ranges of the mesophase stability ($\Delta T=T_i-T_m$) for saturated and unsaturated compounds are listed in Table 4. The variation of the ΔT values for a given

Table 4 Temperatures of the solid→mesophase transitions (T_m) and of the mesophase→liquid transitions (T_i) for the H_2(OASPz) and M(OASPz) compounds and, in parentheses, for the corresponding saturated compounds, when available. Data for saturated compounds are taken from ref. 2(*m*)[a,b]

	H_2			Co			Cu			Ni		
n	T_m/°C	T_i/°C	(T_i-T_m)/°C	T_m/°C	T_i/°C	(T_i-T_m)/°C	T_m/°C	T_i/°C	(T_i-T_m)/°C	T_m/°C	T_i/°C	(T_i-T_m)/°C
4	125.8	154.7	28.9	64.9	237.2[b]	172.3	98.2	220.0[b]	121.8	160.4	217.8	57.4
	(113.1)[a]	(121.9)	(8.8)	(96.0)	(271.0)	(175.0)	(111.7)[a]	(222.8)	(111.1)	(116.9)	(183.5)	(66.6)
5	73.6[a]	107.2	33.6	52.8[a]	246.2[b]	193.4	72.0[a]	212.4	140.5	61.5[a]	174.8	113.3
	—	—	—	—	—	—	—	—	—	—	—	—
6	76.5	—	—	63.0	234.8	171.8	67.5	178.8	111.2	62.5	136.3	73.8
	(77.6)[a]	(92.2)	(14.6)	(45.2)	(243.6)	(198.4)	(80.3)	(189.7)	(109.7)	(75.3)	(154.3)	(79.0)
8	71.3	—	—	39.2	193.6	154.4	58.3	131.1	72.7	67.2	89.7	22.5
	(81.5)	—	—	(55.0)	(208.0)	(153.0)	(67.6)[a]	(151.7)	(84.1)	(67.6)	(118.8)	(51.2)

[a]Polymorphism of the solid phase. [b]Sample decomposes.

Table 5 Enthalpy changes of the solid→mesophase transitions (ΔH_m) and of the mesophase→liquid transitions (ΔH_i) for the H_2(OASPz) and M(OASPz) compounds and, in parentheses, for the corresponding saturated compounds, when available. Data for saturated compounds are taken from ref. 2(*m*)[a,b]

	H_2		Co		Cu		Ni	
n	ΔH_m/J g^{-1}	ΔH_i/J g^{-1}	ΔH_m/J g^{-1}	ΔH_i/J g^{-1}	ΔH_m/J g^{-1}	ΔH_i/J g^{-1}	ΔH_m/J g^{-1}	ΔH_i/J g^{-1}
4	43.0	8.1	13.5	—[b]	7.2	—[b]	7.4	5.2
	(15.7)	(7.4)	(8.19)	—[b]	(15.5)	(11.7)	(16.3)	(11.0)
5	17.4[a]	3.2	10.1[a]	—[b]	40.2[a]	7.9	37.6[a]	5.4
	—	—	—	—	—	—	—	—
6	37.2	—	13.6	2.3	38.3	5.8	15.6	1.5
	(56.2)	(4.6)	(33.2)	(10.5)	(58.7)	(10.7)	(57.8)	(8.7)
8	55.1	—	25.4	1.9	63.0	5.3	36.4	1.2
	(101.0)	—	(37.1)	(9.3)	(99.6)	(8.6)	(93.6)	(7.3)

[a]Polymorphism of the solid phase. [b]Value not available owing to decomposition of the sample.

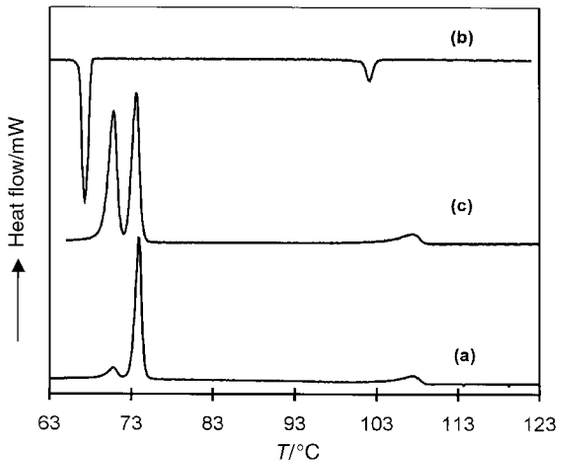

Fig. 3 DSC thermograms of H_2(OASPz) ($n=5$). (a) First heating curve of a solution crystallized sample with no thermal treatment, scan rate 10 °C min^{-1}; (b) first cooling curve, scan rate 5 °C min^{-1}; (c) second heating run, *i.e.* heating curve of the melt crystallized sample, scan rate 10 °C min^{-1}.

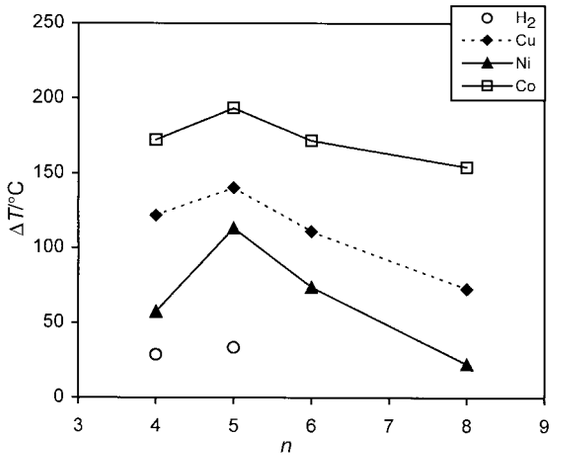

Fig. 4 Thermal range $\Delta T=(T_i-T_m)$ of the mesophase stability for the M(OASPz) and H_2(OASPz) compounds as a function of the number (n) of carbon atoms in the unsaturated aliphatic chains.

metal as a function of the number (n) of the carbon atoms in the unsaturated chains is also shown in Fig. 4.

As inferred from Fig. 4, the ΔT values for the Co derivatives are by far the largest. They are at least 50 °C larger than the Cu ΔT values and even larger than the Ni and free-base ΔT values. Furthermore, for a given coordinated metal, the larger the number of the carbon atoms in the side chains the lower is the thermal range of the mesophase stability.

Although apparently similar trends were found in the parent complexes with saturated peripheral chains, subtle, but not negligible differences are observed upon deeper analysis. Looking at the data reported in Table 4 one may note that for the cobalt complexes the ΔT values are very similar in both classes of complexes (for example, $\Delta T_{unsat}=154.4$ °C and $\Delta T_{sat}=153.0$ °C, for $n=8$). This results from the concomitant decrease of both T_i and T_m values for the complexes with unsaturated chains. Furthermore, from Table 4 it is apparent that in the unsaturated Co porphyrazines the T_i and T_m values do not change significantly going from $n=4$ to 6, but decrease by a considerable extent for $n=8$.

As for the Cu and Ni unsaturated complexes, these show increased narrowing of the ΔT stability range relative to the parent saturated porphyrazines: for example, for $n=8$, for the Cu complexes $\Delta T_{unsat}=72.7$ °C and $\Delta T_{sat}=84.1$ °C; for the Ni complexes $\Delta T_{unsat}=22.5$ °C and $\Delta T_{sat}=51.2$ °C. This reduction of the ΔT is a consequence of the decrease of the temperatures T_i rather than of the increase of the temperatures T_m. Interestingly, unlike the cobalt complexes, the dependence of T_i on n is large for the Cu complexes and even more so for the Ni and H_2 compounds. The value of T_i is lowered at an increasing rate on going from Cu to Ni to H_2 with increasing n.

Summarising, for a given chain size, the double bond has relatively little impact on the mesomorphic behavior of the Co complexes whereas there is a marked effect for Cu, Ni and metal-free porphyrazines which increases in this order. Furthermore, for a given metal, the smaller the n value the smaller is the decrease of T_i.

As inferred from Table 5, where the enthalpy data for saturated and unsaturated porphyrazines are reported, one may observe, for the unsaturated compounds, a general decrease of the ΔH_m and ΔH_i values with respect to the corresponding compounds having saturated peripheral chains. This lowering, which is more evident for the ΔH_i values, is probably due to the weakening, induced by the presence of the terminal double bond in the chains, of the inter-ring interactions both in the solid and liquid-crystalline state.

As expected, and, as found for saturated compounds, the ΔH_i values decrease with n for a given series of unsaturated porphyrazines.

Characterization of the mesophases

The identity of the mesophases exhibited by the present compounds has been assigned on the basis of the appearance of the optical texture when the sample is placed between two crossed polarizers and subsequently confirmed by X-ray data. Well formed and significant optical textures occurred especially on cooling the isotropic liquid between two microscope cover slides, a suitable procedure to prevent the sample from undergoing mechanical stress. The mesogenic metal free porphyrazines show a texture that is indicative of a discotic nematic mesophase. This assignment is also confirmed by X-ray diffraction patterns of the mesophases. For H_2(OASPz) with $n=4$, for example, a diffuse halo at 0.032 Å^{-1} sin ϑ/λ (15.6 Å), suggesting a non-regular packing of the columns, is observed.[2m] Furthermore, the absence of sharp Bragg lines at high angles suggests a disordered stacking of molecules along the columnar axis.

A fan texture is exhibited by the liquid crystalline phases the X-ray diffraction patterns of which indicate hexagonal columnar packing. Such a texture is shown, for example, by Ni(OASPz) with $n=6$ at 92.5 °C. The corresponding X-ray diffraction pattern shows three low angle Bragg lines at d values in the ratio 1 : 0.560 : 0.496 (calculated for hexagonal packing: 1 : 0.577 : 0.500 for planes having Miller indices 10, 11, 20, respectively). No sharp Bragg diffraction lines are observed at high angles indicative that the stacking of the molecules along the columns is disordered.

In all other cases, either arced fan [as for Cu(OASPz) with $n=6$ at 166.8 °C] or spherulitic textures [as for Cu(OASPz) with $n=5$ at 135.6 °C] are observed.

Some evidence of polymorphic behavior in the mesomorphic state has been found for the copper complexes with $n=4$ and 8. The DSC heating curve of solution-crystallized Cu(OASPz) with $n=4$ shows two endothermic peaks at 98.2 and 120.0 °C corresponding to the solid→mesophase 1 and to mesophase 1→mesophase 2 transitions, respectively. As inferred from the X-ray data, mesophase 1 is characterized by a non-hexagonal two dimensional arrangement of the columns. In particular, the pattern shows only one low angle Bragg line at 0.045 Å^{-1} sin ϑ/λ (11.1 Å) and the inner diffraction ring, which in contrast to the single corresponding ring in the hexagonally packed structures, is clearly split in three regions of different intensity. The diffraction spectrum, moreover, shows two Bragg lines at high angles. The first at 0.108 Å^{-1} sin ϑ/λ (4.6 Å) corresponds to the

diffraction of the aliphatic tails while a sharp line at 0.125 $Å^{-1}$ sin ϑ/λ (4.0 Å) is consistent with a stacking periodicity along the columnar axis. Moreover, the macrocyclic cores form a tilting angle of 29.8° with the aliphatic chains to avoid a packing of the side chains which would lead to empty spaces between the aromatic cores. By contrast, no Bragg lines were detectable at higher angles for mesophase 2.

For the Cu(OASPz) complex with $n=8$, observation by light polarized microscopy during the cooling run of the isotropic liquid revealed a textural mesomorphic change. The compound, in the liquid state, shows at 130.0 °C a transition to the mesophase the texture of which is shown in Fig. 5. On further cooling, at 63.0 °C the texture resembles that of a different discotic mesophase as indicated in Fig. 6. This transition, which is readily detected by polarizing microscopy because of sharp texture changes, was not observed by DSC probably as a result of the low transition enthalpy or a second order phase transition (see Fig. 7). The X-ray diffraction pattern characterizing the higher temperature liquid-crystalline phase, contains three sharp Bragg equatorial lines that are assigned as the 10, 11, 20 points of a two dimensional hexagonal lattice. No Bragg diffraction line was observed at high angles but only a diffuse halo at 0.115 $Å^{-1}$ sin ϑ/λ (4.3 Å). We characterized this mesophase as discotic hexagonal disordered.

The same results were obtained for the cobalt and nickel complexes with $n=8$. In particular, the lattice distances corresponding to the low angle Bragg lines are in the ratio 1 : 0.571 for Co and 1 : 0.590 : 0.507 for Ni: this suggests these diffraction lines as the 10, 11 and 10, 11, 20 points of two dimensional hexagonal lattices, respectively.

The small dependence of the lattice distances on the nature of the metal atom for compounds with equal n is consistent with a columnar packing in which the intercolumnar distances are only defined by the cross section of the ligand. Moreover, it was observed that these distances increase linearly with n. These features and the fact that the intercolumnar distances, for compounds with equal n are, for chains with a double bond, only slightly shorter (*ca.* 0.7 Å) than the intercolumnar distances observed for saturated chains, are consistent with a columnar packing of disc-shaped molecules whose basal area increases with increasing number of methylenic groups.

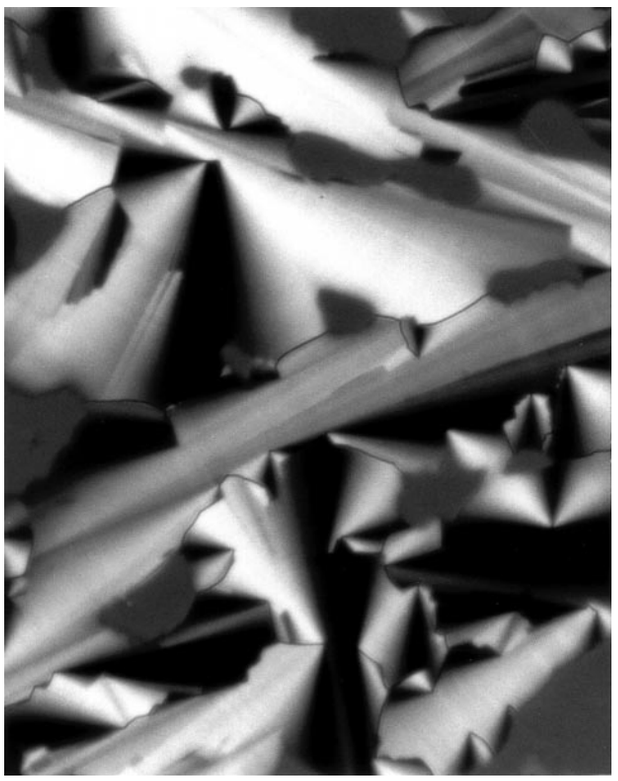

Fig. 5 Liquid-crystalline texture shown by Cu(OASPz) ($n=8$) on cooling the liquid phase at 121.4 °C; crossed polarizers microscope.

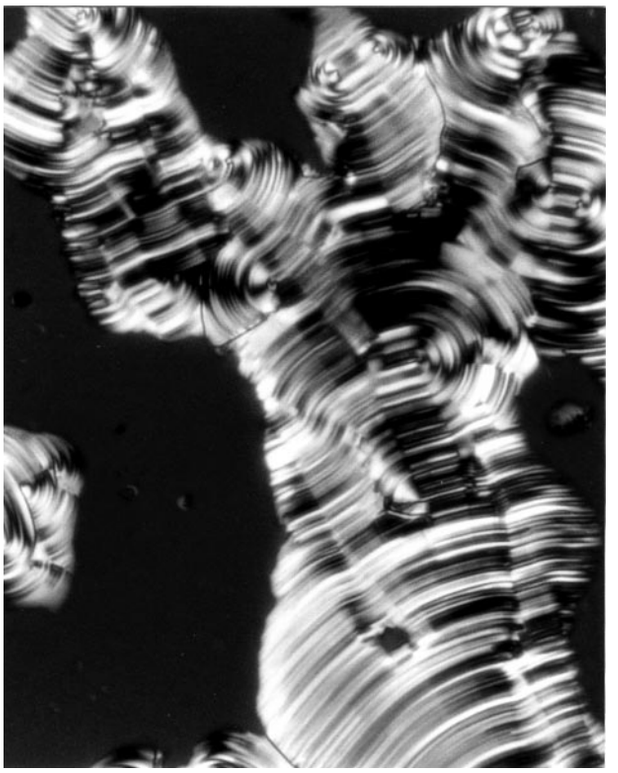

Fig. 6 Liquid-crystalline texture shown by Cu(OASPz) ($n=8$) on cooling at 54.3 °C the mesophase whose texture is shown in Fig. 5; crossed polarizers microscope.

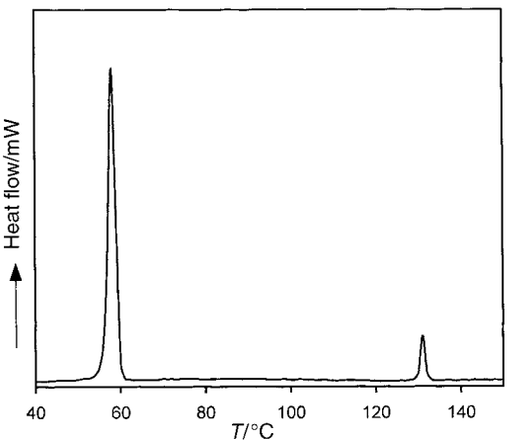

Fig. 7 DSC thermograms of Cu(OASPz) ($n=8$). First heating curve of a solution crystallized sample with no prior thermal treatment. Scan rate 10 °C min^{-1}.

Conclusions

The mesomorphic behavior of a family of newly synthesized 'free-base' and cobalt, copper and nickel alkenyl(sulfanyl)porphyrazines has been investigated and the mesophases characterized by DSC and optical microscopy and for selected compounds, by X-ray diffraction measurements.

It is found that the increase of the chain stiffness, a feature obtained by introducing a terminal double bond in the peripheral chains, has non-negligible effects on the mesomorphism of the studied tetrapyrroles. The terminal double bond reduces the thermal range in which the mesophases are

stable with T_i values of the studied complexes being lower than those of the complexes with saturated side chains. This is in substantial agreement with recent experimental and theoretical studies concerning the role of the stiffness of peripheral chains on the mesomorphism of disklike molecules.[25] This effect is particularly strong for 'free-base', nickel and copper porphyrazines but significantly weaker for cobalt porphyrazines.

The stability order of the mesophases in these compounds is dependent on the coordinated metal. Thermal data indicate that the cobalt complexes show the largest values of T_i and the largest thermal stability ranges of the mesophase in comparison with the other studied compounds. This seems to be consistent with axial Co···S inter-ring interactions, already observed in the crystal phase, operating also within the columns in the LC phase. Further support to a possible role of metal–sulfur inter-ring interactions comes by the fact that 'free-base' porphyrazines, where similar axial interactions are absent, are usually not mesogenic, or at best show nematic mesophases with lower thermal ranges of stability among the investigated porphyrazine compounds.

We can conclude that, when the intracolumnar M···S interactions are effective, as is the case for cobalt, the influence of the nature of the peripheral chains is less relevant to the mesomorphic aggregations.

Although we agree with the assumption that the structure in the crystal being closely related to that in the mesophase is not always valid (EXAFS or similarly sophisticated measurements would be required to check for detectable changes in bond lengths on going from the crystal to the mesophase), nevertheless our data suggest that the M···S interactions observed in the crystal are still operative in the mesophase, especially when, as for Co, the metal shows axial unsaturation, and that such interactions counterbalance the effects of the side chains. Therefore, a subtle interplay between the effects of axial inter-ring interactions and the effects of the nature of the peripheral tails accounts for the observed differences in destabilization of the mesophases in going from one compound to another.

In all, our results indicate that the terminal double bond in the peripheral chains does not preclude the presence of stable mesophases and may lead to applications of these compounds as precursors of polymeric liquid crystals. Polymerization studies are under way in our laboratory and the results will be published elsewhere.

Acknowledgements

Thanks are due to Mr C. Barlabà for technical support and to Mr S. Laurita for collecting X-ray data. Financial support provided by the Advanced Materials Laboratory (LaMI) under the auspices of the European Union and Regione Basilicata and by the Ministero dell'Università e della Ricerca Scientifica e Tecnologica (MURST) is gratefully acknowledged.

References

1 N. Kobayashi, in *Phthalocyanines, Properties and Applications*, ed. C. C. Leznoff and A. B. P. Lever, VCH, New York, 1993, vol. 2.
2 (*a*) J. Fitzgerald, B. S. Haggerty, A. N. Rheingold and L. May, *Inorg. Chem.*, 1992, **31**, 2006; (*b*) N. Yaping, J. Fitzgerald, P. Carroll and B. B. Wayland, *Inorg. Chem.*, 1994, **33**, 2029; (*c*) A. Ghosh, J. Fitzgerald, P. G. Gassman and J. Almolof, *Inorg. Chem.*, 1994, **33**, 6057; (*d*) C. J. Schramm and B. M. Hoffman, *Inorg. Chem.*, 1980, **19**, 383; (*e*) G. Bahr and G. Schleiter, *Chem. Ber.*, 1957, **90**, 438; (*f*) C. S. Velàzquez, G. A. Fox, E. Broderick, K. A. Andersen, O. P. Anderson, A. G. M. Barrett and B. M. Hoffman, *J. Am. Chem. Soc.*, 1992, **114**, 7416; (*g*) F. Bonosi, G. Ricciardi, F. Lelj and G. Martini, *J. Phys. Chem.*, 1993, **97**, 9181; (*h*) F. Bonosi, G. Ricciardi, F. Lelj and G. Martini, *J. Phys. Chem.*, 1994, **98**, 10613; (*i*) G. Ricciardi, F. Lelj and F. Bonosi, *J. Phys. Chem.*, 1993, **215**, 541; (*j*) F. Bonosi, F. Lelj, G. Ricciardi and G. Martini, *Thin Solid Films*, 1994, **243**, 335; (*k*) F. Bonosi, G. Ricciardi and F. Lelj, *Thin Solid Films*, 1994, **243**, 310; (*l*) G. Morelli, G. Ricciardi and A. Roviello, *Chem. Phys. Lett.*, 1991, **185**, 468; (*m*) F. Lelj, G. Morelli, G. Ricciardi, A. Roviello and A. Sirigu, *Liq. Cryst.*, 1992, **12**(6), 941.
3 (*a*) G. Ricciardi, S. Belviso, M. D'Auria and F. Lelj, *J. Porphyrins Phthalocyanines*, 1998, **2**, 517; (*b*) M. D'Auria and F. Lelj, unpublished results.
4 G. Ricciardi, S. Belviso, S. Ristori and F. Lelj, *J. Porphyrins Phthalocyanines*, 1998, **2**, 177.
5 G. Ricciardi, L. De Benedetto and F. Lelj, *Polyhedron*, 1996, **15**, 3183.
6 N. Kobayashi, J. Rizhen, S. Nakajima, T. Osa and H. Hino, *Chem. Lett.*, 1993, **1**, 185.
7 R. Bonnett, *Chem. Soc. Rev.*, 1995, 19.
8 G. Ricciardi, A. Bavoso, A. Bencini, A. Rosa, F. Lelj and F. Bonosi, *J. Chem. Soc., Dalton Trans.*, 1996, 2799.
9 N. Kobayashi, S. Nakajima and T. Osa, *Chem. Lett.*, 1992, **12**, 2410 and references therein.
10 G. Ricciardi, A. Rosa, I. Ciofini and A. Bencini, *Inorg. Chem.*, 1999, **38**, 1422; G. Ricciardi, A. Bencini, A. Bavoso, A. Rosa and F. Lelj, *J. Chem. Soc., Dalton Trans.*, 1996, 3243.
11 A. M. Giroud-Godquin and P. M. Maitlis, *Angew. Chem., Int. Ed. Engl.*, 1991, **30**, 375.
12 D. M. Knawby and T. M. Swager, *Chem. Mater.*, 1997, 535.
13 J. Martinsen, J. L. Stanton, R. L. Greena, J. Tanaka, B. M. Hoffman and J. Ibers, *J. Am. Chem. Soc.*, 1985, **107**, 6915.
14 F. Wudl, *Acc. Chem. Res.*, 1984, **17**, 227.
15 M. Sato, A. Takeuchi, T. Yamada, H. Hoshi, K. Ishikawa, T. Mori and H. Takezoe, *Phys. Rev. E*, 1997, **56**, 6.
16 G. Serrano, in *Metallomesogens*, VCH, Berlin, 1995.
17 S. Chandrasekhar, in *Liquid Crystals*, Cambridge University Press, 2nd edn., 1992.
18 D. Demus, J. Goodby, G. W. Gray, H. W. Spiess and V. Vill, in *Handbook of Liquid Crystals*, Wiley–VCH, 1998, vol. 2B.
19 J. Simon and P. Bassoul, in *Phthalocyanines, Properties and Applications*, ed. C. C. Leznoff and A. B. P. Lever, VCH, New York, 1993, vol. 2.
20 B. A. Gregg, A. M. Fox and A. J. Bard, *J. Am. Chem. Soc.*, 1989, **111**, 3024.
21 K. Ohta, M. Ando and I. Yamamoto, *J. Porphyrins Phthalocyanines*, 1999, **3**, 249.
22 W. Kreuder and H. Ringsdorf, *Makromol. Chem. Rapid Commun.*, 1983, **4**, 807.
23 W. Kreuder, H. Hingsdorf and P. Tschirner, *Makromol. Chem. Rapid Commun.*, 1983, **6**, 387.
24 D. Demus, J. Goodby, G. W. Gray, H. W. Spiess and V. Vill, in *Handbook of Liquid Crystals*, Wiley–VCH, 1998, vol. 3 and vol. 2B, ch. VIII.
25 M. Wnek and J. K. Moscicki, *Phys. Rev. E*, 1999, **59**, 535.

Paper a907498h